The Astrophysical Journal, 668: L75–L78, 2007 October 10

ORGANIC VOLATILES IN COMET 73P-B/SCHWASSMANN-WACHMANN 3 OBSERVED DURING ITS OUTBURST: A CLUE TO THE FORMATION REGION OF THE JUPITER-FAMILY COMETS[1]

Hitomi Kobayashi,[2] Hideyo Kawakita,[2,3] Michael J. Mumma,[4] Boncho P. Bonev,[4]
Jun-ichi Watanabe,[5] and Tetsuharu Fuse[5]

Received 2007 June 17; accepted 2007 August 17; published 2007 September 25

ABSTRACT

We report the chemical composition of organic molecules in fragment B of comet 73P/Schwassmann-Wachmann 3 (SW3). Comet SW3 is a Jupiter-family comet that split into three fragments during its 1995 apparition and later into additional components. It was expected that fresh ices from deep within the presplit nucleus were exposed on the surface of each fragment. We observed SW3 with the Subaru telescope in 2006 early May when component B was disintegrating rapidly. If this exposed fresh ices from deeper layers of the original nucleus, mixing ratios obtained from our observations may reflect the pristine nature of the comet. Based on our results, comet SW3-B was depleted in C_2H_6 and C_2H_2 with respect to most comets from the Oort Cloud reservoir, suggesting its formation region might have differed from that of the dominant Oort Cloud comets. Furthermore, the chemical composition of SW3-B was similar to that of SW3-C, suggesting that the presplit nucleus was almost homogeneous in volatile composition. The combined results demonstrate that depleted-organics comets from a common formation zone entered both reservoirs, of Jupiter-family comets and and Oort Cloud comets, but likely in different fractions.

Subject headings: comets: individual (73P-B/Schwassmann-Wachmann 3) — Kuiper Belt — solar system: formation

Online material: color figure, machine-readable table

1. INTRODUCTION

Comets today reside in two distinct reservoirs, the Oort Cloud and the Kuiper Belt region (divided into the classical Kuiper Belt, the scattered disk, and the extended scattered disk). Comets injected into the inner planetary system are grouped dynamically into several orbital categories: isotropic (dynamically new, long-period, Halley type), and ecliptic (Centaur type, Encke type, and Jupiter-family comets, hereafter JFCs).

Most JFCs likely come from the scattered disk (Bernstein et al. 2004). Their original formation region is less clear. It once was thought that most JFCs formed in the Kuiper Belt region ($R_h >$ 30 AU) while Oort Cloud comets (OCs) formed in the giant planets region (5–30 AU) of the protoplanetary disk. Following this paradigm, the OCs formed in warmer regions than the JFCs; thus, some differences in chemistry or dust properties should be found between JFCs and OCs but each reservoir would contain distinct chemical populations. A new paradigm has been proposed (the "Nice" model) and it predicts that comets formed in the outer protoplanetary disk (10–30 AU) entered both the Oort Cloud and the Kuiper disk, although likely in different proportions (Crovisier 2007; Morbidelli 2005). A comparison of chemical taxonomies in JFC and OC populations might test a possible radial gradient in the chemistry of icy planetesimals in the protoplanetary disk, and the dynamical models that predict their dissemination. Although A'Hearn et al. (1995) reported that about one-half of the sampled JFCs were depleted in C_2 and C_3 relative to CN based on the observations of daughter species in 85 comets, the parentage of these daughter species is often uncertain. A taxonomy based on direct measurement of parent volatiles is required.

Direct observational measurements (from molecular spectroscopy) of parent volatiles among JFCs and OCs are expanding rapidly and already have revealed two distinct classes based on their organic chemistry ("normal" and depleted) (Crovisier 2007; Bockelee-Morvan et al. 2004; Mumma et al. 2003). The controlled *Deep Impact* event was designed to test whether the surface material of this JFC was modified by thermal fractionation while in the inner solar system. It revealed (A'Hearn et al. 2005) that material ejected from the nucleus of 9P/Tempel 1 (a JFC) was similar in composition to organics-normal OCs, even though material released during the quiescent phase was organics-depleted (e.g., depleted in ethane; Mumma et al. 2005). Mumma et al. argued that the difference could be interpreted in two ways: (1) internal heterogeneity resulting from radial migration of dissimilar planetesimals before aggregation, or (2) depletion of the surface layer by solar heating during prior apparitions.

In order to constrain the above paradigms, we need additional opportunities to investigate the inner materials of cometary nuclei. Fortunately, split comets provide a natural means to this end by exposing fresh materials (originally hidden in the parent nucleus) on the surface of the fragments. The JFC 73P/Schwassmann-Wachmann 3 (SW3) split into three components (A, B, and C) in the 1995 apparition, and more components were found later (Sekanina 2005). SW3 has an orbital period of about 5.4 yr, and its apparition in 2006 was eagerly awaited owing to its very close approach to Earth.

Component B was particularly active in 2006, showing frequent outbursts and fragmentations (Weaver et al. 2006; Fuse et al. 2007; ICQ reports). The repeated outbursts provided a precious opportunity to investigate fresh ices in the nucleus (Fernandez 2005; Boehnhardt 2004). Before these outburst phenomena, the surface might have been covered by debris processed by solar heating during the previous apparition in 2001.

[1] This Letter is based on data collected at Subaru Telescope, which is operated by the National Astronomical Observatory of Japan. This work was financially supported by the Ministry of Education, Science, and Culture, Grant-in-Aid for Young Scientists 19740107 (H. K.).

[2] Department of Physics, Faculty of Science, Kyoto Sangyo University, Motoyama, Kamigamo, Kita-ku, Kyoto 603-8555, Japan.

[3] Corresponding author; kawakthd@cc.kyoto-su.ac.jp.

[4] NASA Goddard Space Flight Center, Greenbelt, MD 20771.

[5] National Astronomical Observatory of Japan.

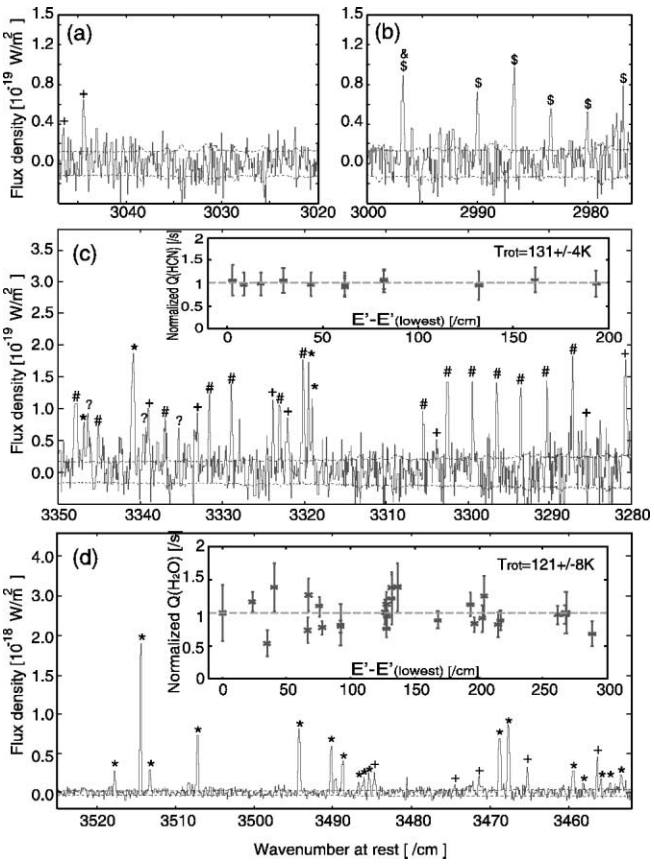

FIG. 1.—Selected spectra of molecular emission from comet SW3-B on May 9 UT. Flux densities are observed at the ground. The sunlight reflected by cometary dust grains has been removed as a continuum component from each spectrum considering telluric atmosphere transmittance. The $\pm 1\ \sigma$ error levels are shown by dotted lines. Asterisks (*), plus signs (+), pound signs (#), dollar signs ($), and ampersands (&) correspond to H_2O, OH, HCN, C_2H_6, and CH_3OH, respectively. Some unknown lines are marked by a question mark (?). Panel *a* shows methane region [including positions of CH_4 v_3 $R(0)$ and $R(1)$ lines] but no obvious lines of CH_4. Although there are some line positions of C_2H_2 in (*c*), no clear emission lines of C_2H_2 are recognized in the spectrum. Insets show the production rates derived from individual lines of HCN and H_2O (error bars correspond to $\pm 2\ \sigma$ levels), from which the optimum rotational temperatures were derived (Table 2). [*See the electronic edition of the Journal for a color version of this figure.*]

2. OBSERVATIONS AND PIPELINE DATA REDUCTION

Near-infrared spectroscopic observations of component B were acquired on 2006 May 9 and 10 UT using the 8 m Subaru telescope with the Infrared Camera and Spectrograph (IRCS; Kobayashi et al. 2000) located atop Mauna Kea, Hawaii. The IRCS instrument has three observational modes: imaging, grism spectroscopy, and cross-dispersed echelle spectroscopy. The cross-dispersed echelle mode provides the highest resolving power, so we used it for spectral observations.

The comet parameters (heliocentric distance [AU], geocentric distance [AU], geocentric velocity [km s^{-1}]) were (1.03, 0.078, −7.4) on May 9.5 UT and (1.03, 0.074, −6.4) on May 10.5 UT. A photometric standard star (BS 7178; spectral type B9 III) was observed for flux calibration. The sizes of slits were $9.5'' \times 0.27''$ ($\lambda/\delta\lambda \sim 10^4$) for the comet and $9.5'' \times 0.54''$ ($\lambda/\delta\lambda \sim 5 \times 10^3$) for the standard star. The comet (or the standard star) was centered on the slit and nodded between two different positions (A and B, separated by 5″) in a dithering sequence of ABBA. We used two grating settings on May 9 (three on May 10) to cover as many molecular emission lines as possible. The total integration times on the comet were 720 s (spanning May 9.54–9.58) and 1920 s (spanning May 10.47–10.62), respectively.

TABLE 1
MEASURED MOLECULAR EMISSION LINES

Upper State (v_1, v_2, v_3) $J_{Ka\,Kc}$	Lower State (v_1, v_2, v_3) $J_{Ka\,Kc}$	Wavenumber (Rest) (cm^{-1})	Flux, May 9 UT (W m^{-2})	Flux, May 10 UT (W m^{-2})
	H_2O			
(1, 0, 1) $2_{2\,1}$	(1, 0, 0) $3_{2\,2}$	3517.70	5.69E−19	1.68E−19
(1, 0, 1) $2_{1\,1}$	(1, 0, 0) $3_{1\,2}$	3514.41	4.36E−18	1.36E−18
(1, 0, 1) $2_{2\,0}$	(1, 0, 0) $3_{2\,1}$	3513.21	6.52E−19	…

NOTE.—Table 1 is published in its entirety in the electronic edition of the *Astrophysical Journal*. A portion is shown here for guidance regarding its form and content.

Raw data were processed using the Image Reduction and Analysis Facility (IRAF) software package distributed by the National Optical Astronomy Observatory (NOAO). For each sequence of ABBA, we calculated (A − B − B + A) to cancel the sky background emission. Wavelength calibration and resampling of spectra were performed by comparing measured background sky emission lines and modeled atmospheric radiance spectra. Stellar fluxes were corrected for slit losses (the stellar PSF was measured along the slit, and the FWHM was ∼0.4″ on May 9 and 10 UT). The cometary (reflected solar) continuum was removed by fitting the synthesized atmospheric transmittance (modeled using the LBLRTM code [Clough & Iacono 1995], which accesses the HITRAN molecular database) to regions without emission lines. Each cometary line flux extracted from the residual spectrum was corrected for telluric extinction at its Doppler-shifted wavelength using the fully resolved transmittance function. The final cometary emission spectra are shown in Figure 1 and the detected emission lines are listed in Table 1 (comet signals were extracted from an aperture [$0.27'' \times 0.27''$] centered on the nucleus). Additional details of our observing procedure and data analysis are given elsewhere (Kawakita et al. 2006).

3. SPECTRAL ANALYSIS AND EXTRACTION OF QUANTITATIVE RESULTS

The high spectral and spatial resolution afforded by IRCS permitted extraction of molecular rotational temperatures and production rates, quantifying the chemical composition of comet SW3-B. We assumed the spatial distribution of parent molecules in the coma to be governed by spherically symmetric steady-state production with a constant expansion velocity. Of the molecules sampled by a pencil beam centered on the nucleus, a large fraction ($2/\pi$) lie within the inscribed sphere (i.e., within ∼7 km from the nucleus, under our observing conditions). After release from the nucleus, parent molecules transit the PSF in only ∼14 s (assuming outflow velocity 800 m s^{-1}), much shorter than the limiting temporal resolution of our spectra (each ABBA sequence spanned 4 minutes). Our spectra are strongly influenced by conditions in the highest density (near-nucleus) regions of the inner coma and by the short-term temporal behavior of gas production.

For HCN and H_2O, the rotational population distribution in the ground vibrational state was consistent with a Boltzmann distribution characterized by a specific rotational temperature (T_{rot}), permitting the total population to be calculated from the subset of levels (quantum states) sampled. The rotational temperatures retrieved for H_2O and HCN agree within their confidence limits on each date (Table 2), suggesting that rovibrational distributions for both species were controlled by

TABLE 2
PRODUCTION RATES AND MIXING RATIOS OF PARENT VOLATILES IN SW3-B

Molecule	T_{rot} (K)	Q (molecules s^{-1})	Mixing Ratio (%)	Remarks
		May 9 UT		
H_2O	121 ± 8	(3.5 ± 0.2) × 10^{28}	100.0	
HCN	131 ± 4	(9.5 ± 1.1) × 10^{25}	0.27 ± 0.03	
C_2H_6	(121)	(5.6 ± 0.4) × 10^{25}	0.16 ± 0.01	
C_2H_2	(121)	...	<0.12[a]	v_3 $R(3)$
CH_4	(121)	...	<4.08[a]	v_3 $R(0)$
		May 10 UT		
H_2O	112 ± 5	(1.9 ± 0.2) × 10^{28}	100.0	
HCN	110 ± 8	(6.6 ± 0.7) × 10^{25}	0.35 ± 0.02	
C_2H_6	(112)	(4.2 ± 0.5) × 10^{25}	0.22 ± 0.02	
C_2H_2	(112)	...	<0.18[a]	v_3 $R(3)$
CH_4	(112)	...	<17.7[a]	v_3 $R(0)$

NOTES.—T_{rot} and Q for H_2O are measured after combining all data for a given night. Temporal variability in these parameters within a single night will be investigated in a separate paper.

[a] 3 σ upper limits.

collisions in the inner coma. Radiative cooling is inactive for molecules that lack a dipole moment (e.g., C_2H_6, C_2H_2, and CH_4), so for them collisions are even more effective at controlling the rotational distribution. For them, we adopted the rotational temperature retrieved for H_2O.

Certain vibrational hot bands of water encompass the wavelength range covered by our observations. From each spectral line, we can estimate the total water production rate as follows:

$$Q(\mathrm{H_2O}) = \frac{4\pi\Delta^2}{f_{\mathrm{geom}}\tau_{\mathrm{H_2O}}}\frac{F}{g} = \frac{8\pi\Delta\, v_{\mathrm{exp}}}{\theta_1 \arcsin(\theta_2/\theta_1) + \theta_2 \arcsin(\theta_1/\theta_2)}\frac{F}{g}, \quad (1)$$

where $Q(H_2O)$ denotes the water production rate (molecules s^{-1}), Δ denotes the geocentric distance (m), f_{geom} denotes the fraction of water molecules within the observed (slit) aperture, τ_{H_2O} denotes the photodissociation lifetime of water (~8.33 × 10^4 s at 1 AU for the quiet Sun; see Huebner et al. 1992), F denotes the observed line flux at the top of the atmosphere (J m^{-2} s^{-1}), g denotes the g-factor (emission efficiency) for the spectral line (J s^{-1} $molecule^{-1}$), v_{exp} denotes the outflow velocity (~800 m s^{-1} at 1 AU from the Sun), and θ_1 and θ_2 denote the slit length and slit width, respectively. The values of f_{geom} were estimated to be 2.14 × 10^{-4} and 1.92 × 10^{-4} for May 9 and 10, respectively (following Kawara et al. 1988). The expression of f_{geom} shown by Kawara et al. (1988) is valid only for the case in which both $(\theta_1\Delta)/(v_{exp}\tau_{H_2O})$ and $(\theta_2\Delta)/(v_{exp}\tau_{H_2O}) \ll 1$. In our observations, these conditions were satisfied. In equation (1), the lifetime is canceled and $Q(H_2O)$ depends on the outflow velocity, which is likely the same for all parent volatiles.

The g-factors for H_2O are based on a solar fluorescence model (Dello Russo et al. 2004; Barber et al. 2006) and are sensitive to T_{rot}. The ratio F/g (proportional to the total production rate derived from that line alone) achieves (ideally) a value independent of the spectral line identity if the correct rotational temperature is used. Minimizing the variance in the group (F/g) provides a convenient way to extract the "best" rotational temperature when simple rotation diagrams are not possible (see Dello Russo et al. 2004), e.g., H_2O (Fig. 1). A Q-curve analysis was also performed to correct for slit losses and outflow asymmetries when determining a precise water production rate (Bonev et al. 2006, Appendix B).

Production rates for other species in SW3-B were obtained in the same manner, using parameters appropriate to them (e.g., g-factors, lifetimes). Mixing ratios were obtained by comparing production rates for each species with that of water. Rotational temperatures, production rates, and mixing ratios for SW3-B are listed in Table 2.

4. DISCUSSION

4.1. *Variability of Water Production and the Reliability of Mixing Ratios*

SW3-B was in strong outburst on May 9.5 but the production rate of water $Q(H_2O)$ decreased by about 50% within 24 hr, from 3.5 × 10^{28} on May 9.5 UT to 1.9 × 10^{28} on May 10.5 UT (Table 2). Despite observing SW3-B during an outburst, we expect that our assumptions for the gas outflow result in reasonable production rates and robust mixing ratios. Because of the very small geocentric distance, the slit subtense was only about 15 × 540 km, resulting in a transit time of ~19 (~100) s across (along) the slit for outflow velocity of 800 m s^{-1}. For such short durations the assumption of a steady-state coma is a good approximation, even if it breaks on longer (~day) timescales. Temporal variability of $Q(H_2O)$ within a single night will be discussed in a follow-up paper (B. P. Bonev et al. 2007, in preparation). Here we emphasize that the retrieved mixing ratios are highly robust because the trace species are measured simultaneously with water, and so they are less sensitive to "secular" changes in the total gas production. This is confirmed by the fact that we retrieve very similar mixing ratios on May 9 and 10 UT, despite the apparent ~50% decrease in $Q(H_2O)$.

4.2. *Mixing Ratios of Component B of SW3*

Short-term changes in the chemical composition of volatiles released from SW3-B while in outburst may reveal fundamental information on the internal structure of this fragment. Although the water production rates decreased from May 9.5 to 10.5 UT, the mixing ratios did not change significantly (Table 2). It is interesting to compare our results obtained during and after the outburst to those obtained well before. Together, they can provide a measure of the internal chemical homogeneity of fragment B.

Near-infrared spectroscopic observations of components B and C were carried out by Villanueva et al. (2006) using Keck II NIRSPEC at Mauna Kea, Hawaii, in 2006 mid-April. They targeted the abundances of organic molecules as in this Letter. For Fragment B, they reported $Q(H_2O)$ and 3 σ upper limits for mixing ratios of C_2H_6 and HCN (0.3% and 0.2%, respectively). Their upper limit for C_2H_6 is consistent with our results, but their upper limit for HCN is significantly lower than ours. The difference in HCN might originate in heterogeneity of the nucleus B. Gibb et al. (2007) reported day-to-day changes in the mixing ratios (relative to H_2O) of CH_4 and H_2CO in comet C/2001 A2 (LINEAR), which showed frequent outbursts and fragmentations like SW3. Outburst and fragmentation events might be related to such heterogeneity of the chemistry in a comet nucleus. Otherwise, the upper limit of HCN/H_2O ratio reported by Villanueva et al. (2006) might reflect processing of near-surface materials by solar heating since the breakup in 1995.

4.3. *Heterogeneity in the Parent Body of SW3*

Comparison of SW3-B with other fragments of SW3 can establish important limits to the heterogeneity of their parent body

TABLE 3
COMPARISON BETWEEN 73P-B/SW3 AND OTHER COMETS

COMET	H_2O = 100				REMARKS
	HCN	C_2H_6	C_2H_2	CH_4	
SW3-B (May 9 UT)	0.27 ± 0.03	0.16 ± 0.01	<0.12	<4.08	This work
SW3-B (May 10 UT)	0.35 ± 0.02	0.22 ± 0.02	<0.18	<17.7	This work
SW3-B (Apr 15 UT)	<0.2	<0.3	…	…	Villanueva et al. (2006)
SW3-C (Apr 7 UT)	0.17 ± 0.02	0.15 ± 0.04	…	<0.25	Villanueva et al. (2006)
SW3-C (Apr 16 UT)	0.21 ± 0.04	…	0.23 ± 0.06	<0.39	Villanueva et al. (2006)
Typical OCs	0.2–0.3	0.6	0.2–0.3	0.5–1.5	Mumma et al. (2003)
2P/Encke	…	0.3–0.4	…	…	Mumma et al. (2005)
21P/Giacobini-Zinner	…	~0.2	…	…	Mumma et al. (2005)
9P/Tempel 1 (preimpact)	0.18 ± 0.06	0.19 ± 0.04	…	…	Mumma et al. (2005)
9P/Tempel 1 (ejecta only)	…	0.59 ± 0.18	…	…	Mumma et al. (2005)

(Crovisier 2007). There are no remarkable differences between components B (this work) and C (Villanueva et al. 2006). Even though Villanueva et al. (2006) reported higher C_2H_2 mixing ratio in C than we report for B, it is difficult to draw strong conclusions owing to the modest confidence limits. Thus, we conclude that the parent body of SW3 could be almost homogeneous and it might be an aggregate of planetesimals formed locally in the solar nebula (or formed under similar environments).

4.4. *Comparison of SW3-B with other JFCs and OCs*

We also compare the mixing ratios of SW3-B with other JFCs and OCs (Table 3). Moderate depletion in C_2H_6 and strong depletion in C_2H_2 with respect to the "typical" composition of OCs should be noted. Given that we observed SW3-B during its outburst and that we consider the derived mixing ratios to be primordial, SW3-B must have contained icy materials formed in an environment different from that of the typical OCs. Models for physicochemical evolution of icy mantles on grains in the solar nebula predict that molecular abundance ratios of ices vary significantly with heliocentric distance. A plausible scenario for the origin of the SW3 ices is that they formed from previously sublimated material that was chemically modified in the gas phase at small heliocentric distances and subsequently recondensed in the 5–10 AU range as proposed for the OC comet C/1999 S4 (LINEAR), which also displayed a depleted organic chemistry (Mumma et al. 2001). We point out that measurements of isotopic abundances (D/H) in future comets with similar (to SW3) volatile composition would be helpful tests of this formation scenario.

Some JFCs are also depleted in C_2H_6 (see Table 3), but the number sampled is not yet sufficient to reveal whether the depletion in C_2H_6 is a typical signature for JFCs or not. The depletion of C_2H_6 in both some JFCs and C/1999 S4 (an OC) might be the signature of injection to both reservoirs (albeit in different fractions) of comets formed in the warm 5–10 AU region of the protoplanetary disk.

In interpreting comet volatile composition, we point out that some comets might be aggregates of planetesimals formed under various conditions in the solar nebula. Possible heterogeneity of the Tempel 1 nucleus in C_2H_6/H_2O (Mumma et al. 2005) and CO_2/H_2O (Feaga et al. 2007) abundance ratios supports this hypothesis

5. CONCLUSIONS

Our conclusions are as follows:

(1) We propose the hypothesis that the formation region of SW3-B was different from that of typical OCs. We suggest the hypothesis of formation region of SW3-B was 5–10 AU in the protoplanetary disk, similar to the formation region of S4/LINEAR.

(2) The parent nucleus of SW3 was relatively homogeneous and the nucleus was an aggregate of planetesimals that formed locally (in similar environments) in the protoplanetary disk.

(3) The depletions in C_2H_6 found in SW3-B and C (and likewise in some other JFCs) are similar to the depletion of C_2H_6 found in C/1999 S4 (an OC). This might be the signature of injection of comets formed in the warm 5–10 AU region of the protoplanetary disk into both the scattered disk and the Oort Cloud (probably in different fractions).

REFERENCES

A'Hearn, M. F., et al. 1995, Icarus, 118, 223
———. 2005, Science, 310, 258
Barber, R. J., et al. 2006, MNRAS, 368, 1087
Bernstein, G. M., et al. 2004, AJ, 128, 1364
Bockelée-Morvan, D., Crovisier, J., Mumma, M. J., & Weaver, H. A. 2004, in Comets II, ed. M. Festou et al. (Tucson: Univ. Arizona Press), 391
Boehnhardt, H. 2004, in Comets II, ed. M. Festou et al. (Tucson: Univ. Arizona Press), 301
Bonev, B. P., et al. 2006, ApJ, 653, 774
Clough, S. A., & Iacono, M. J. 1995, J. Geophys. Res., 100, 16519
Crovisier, J. 2007, in Proc. 18th Rencontres de Blois: Planetary Science: Challenges and Discoveries, in press (astro-ph/0703785)
Dello Russo, N., et al. 2004, Icarus, 168, 186
Feaga, L. M., A'Hearn, M. F., Sunshine, J. M., Groussin, O., & Farnham, T. L. 2007, Icarus, in press
Fernandez, J. A. 2005, Comets (Dordrecht: Springer)
Fuse, T., et al. 2007, PASJ, 59, 381
Gibb, E. L., et al. 2007, Icarus, 188, 224
Huebner, W. F., Keady, J. J., & Lyon, S. P. 1992, Ap&SS, 195, 1
Kawakita, H., et al. 2006, ApJ, 643, 1337
Kawara, K., Gregory, B., Yamamoto, T., & Shibai, H. 1988, A&A, 207, 174
Kobayashi, N., et al. 2000, Proc. SPIE, 4008, 1056
Morbidelli, A. 2005, preprint (astro-ph/0512256v1)
Mumma, M. J., et al. 2001, Science, 292, 1334
———. 2003, Adv. Space Res., 31, 2563
———. 2005, Science, 310, 270
Sekanina, Z. 2005, Int. Comet Q., 27, 225
Villanueva, G. L., et al. 2006, ApJ, 650, L87
Weaver, H. A., et al. 2006, BAAS, 38, 490